Published by Institute of Physics Publishing for SISSA/ISAS

Received: *August 19, 2002*
Revised: *September 30, 2002*
Accepted: *October 02, 2002*

NLO corrections to ultra-high energy neutrino-nucleon scattering, saturation and small x

Rahul Basu

The Institute of Mathematical Sciences, C.I.T. Campus
Taramani, Chennai 600 113, India
E-mail: rahul@imsc.ernet.in

Debajyoti Choudhury and Swapan Majhi

Harish-Chandra Research Institute
Chhatnag Road, Jhusi, Allahabad 211 019, India
E-mail: debchou@mri.ernet.in, swapan@mri.ernet.in

Abstract: We reconsider the standard model interactions of ultra-high energy neutrinos with matter. The next to leading order QCD corrections are presented for charged-current and neutral-current processes. Contrary to popular expectations, these corrections are found to be quite substantial, especially for very large (anti-) neutrino energies. Hence, they need to be taken into account in any search for new physics effects in high-energy neutrino interactions. In our extrapolation of the parton densities to kinematical regions as yet unexplored directly in terrestrial accelerators, we are guided by double asymptotic scaling in the large-Q^2 and small Bjorken x region and to models of saturation in the low Q^2 and low x regime. The sizes of the consequent uncertainties are commented upon. We also briefly discuss some variables which are insensitive to higher order QCD corrections and are hence suitable in any search for new physics.

Keywords: Deep Inelastic Scattering, NLO Computations, High Energy Cosmic Rays, Neutrino and Gamma Astronomy.

JHEP10(2002)012

Contents

1. Introduction

Ultra-high energy neutrinos and their interactions continue to attract much attention. This is in spite of the fact that no such neutrino has been seen so far (and hence bounds been placed on their fluxes [1]). Much of the continuing interest has been occasioned by the observation, in more than one detector, of ultra-high energy cosmic rays (UHECR). An interaction of such cosmic rays with either the microwave background radiation or even the atmosphere would presumably lead to the generation of charged pions and through their decay, to extremely energetic neutrinos [2]. Alternatively, *primary* ultra-high energy neutrinos themselves could lead to UHECR, thereby avoiding the GZK bound. A possible source for such primary neutrinos is the decay of an extremely massive primordial relic or even a cosmic string [3]. Whatever their origin, it can safely be asserted that cosmic high energy neutrinos are inextricably linked to the very high energy cosmic rays. The experimental detection of such neutrino fluxes is thus expected to provide rare insight into the origin of such cosmic rays and probably to physics beyond the SM as well. Such observations have the additional promise of probing stellar structures [4], for unlike charged particles, cosmic neutrinos do not suffer any bending due to inter-galactic magnetic fields and hence arrive on earth in a direct line from their source.

Consequently, various experimental efforts are being planned. Pilot experiments, based on the optical detection of Čerenkov light emitted by the muons created in charged current reactions of neutrinos with nucleons either in water or in ice, include the Antarctic Muon And Neutrino Detector Array (AMANDA) [5] in the South Pole ice and the one at Lake Baikal [6]. The next generation experiments using similar techniques comprise the Neutrino Telescope and Abyss environmental RESearch (ANTARES) [7], the Neutrino Experiment SouthwesT Of GReece (NESTOR) project in the Mediterranean [8], as well as

JHEP10(2002)012

ICECUBE [9], the proposed kilometer scale version of the AMANDA detector. Recently, arguments have been forwarded in favour of facilities based on the detection of radio pulses emanating from the electromagnetic showers created by neutrino interactions in ice and other materials. The primary advantage of such a technique would be the scalability up to an effective area of $10^4\,\mathrm{km}^2$ and the Radio Ice Cĕrenkov Experiment (RICE) experiment at the South Pole [10] is a functioning prototype. It has also been realized that neutrinos can initiate horizontal Extensive Air Showers (EAS) which could be detected by giant ground arrays and fluorescence detectors such as the cosmic ray Pierre Auger Project [11]. Deeply penetrating EAS could also be detected by observing their fluorescence light from space based instruments such as the Orbiting Wide-angle Light-collector (OWL) [12] and the Extreme Universe Space Observatory (EUSO) [13]. Finally, there is the newly approved balloon experiment ANtartic Impulsive Transient Antenna (ANITA) which will look for radio Cĕrenkov pulses created by ultra-high energy neutrino interactions and emanating from very large chunks of the Antarctic ice cap. Its energy threshold is about $10^{18}\,\mathrm{eV}$, so it will primarily be looking for GZK neutrinos [14].

These experiments, taken together, are sensitive to neutrino energies of up to 10^{11} GeV or so. The actual event rates are somewhat uncertain though, as they depend crucially on both the predicted neutrino fluxes, as well as on the ultra-high energy neutrino cross sections which, for want of a better method, we may only estimate by a reasonable extrapolation beyond the measured regime. The interaction of UHE neutrinos with matter is through deep inelastic scattering of the neutrinos with protons and neutrons. Over the last few years, numerous issues with regard to the nature of the cross section of $\nu - N$ scattering (where N is a proton or a neutron) have gained importance and some of these are discussed in refs. [15, 16, 17].

Most of the discussion on $\nu - N$ scattering has been based on the leading order (LO) expressions for neutrino nucleon scattering (i.e. α_{s} independent). The usual procedure followed has been to use the lowest order parton level cross section and convolute it with the LO or sometimes even next to leading order (NLO) parton distributions. QCD corrections to the partonic cross sections have typically been neglected, in view of the high energies involved and the consequent small value of the strong coupling constant α_{s}. While, at first sight, such an approximation may seem appropriate, it must be borne in mind that the consequent uncertainties may limit the sensitivity of neutrino telescopes [5], [7]–[10] (and to a smaller extent, the cosmic-ray detectors [11, 12, 13]) to physics beyond the standard model. Amongst possible such scenarios, of particular interest are theories with supersymmetry [18], extended gauge or higgs sector [19] or, more recently, those with a low energy gravity sector [20]. Perhaps, of even more importance, are the effects on the determination of neutrino mixing parameters [21], and neutrino-tomography of the earth's interior [22]. The importance of a more accurate estimation of the neutrino interaction rates as well as their kinematical distributions, thus, cannot be overstated.

In this paper, we explicitly calculate the $\mathcal{O}(\alpha_{\mathrm{s}})$ QCD corrections to the parton model result and show that while it is not very large, it is by no means negligible. Moreover, we study carefully the behavior of this correction as a function of neutrino energy and find behavior which is not necessarily very intuitive. For example, there is a delicate interplay

JHEP10(2002)012

between the magnitude of α_s, the structure of the higher order integrals and the size of the parton distributions (particularly the gluon) in LO and NLO. This gives a non-trivial energy dependence to the ratio of the LO and NLO cross section (which we will call the K-factor). We work throughout in the $\overline{MS}$ scheme.

Another issue which is of relevance in these energy ranges (and which, again, has been addressed in refs. [15, 16, 17]) is the question of carrying out perturbative calculations at ultra low Bjorken x (down to 10^{-8}). No data exists to help in parametrisations of parton distribution functions at such values of x and one can only be guided in these regions by a somewhat improperly understood physical picture of a highly dense nucleon of partons. Data from HERA stops around $x \simeq 10^{-5}$ or so and below that, some physical picture of shadowing and saturation effects (particularly at low Q^2) needs to be incorporated to understand the physics of a nucleon with a high density of partons.

We have tried to address both these issues in this paper. We have explicitly calculated the $\mathcal{O}(\alpha_s)$ corrections to the partonic cross sections and convoluted them with appropriate parton distributions. We have also addressed the issue of extrapolation of the partonic distributions to regions where simple DGLAP evolution is not expected to hold.

The paper is organised as follows. In section 2, we present a discussion and justification for the various partonic distributions that we have used in various parts of the (Q^2, x) plane. In section 3, we present detailed expressions for the $\mathcal{O}(\alpha_s)$ corrections to the lowest order partonic cross section for neutrino and antineutrinos scattering against an isoscalar target. These expression are, of course available elsewhere but for the sake of completeness and clarity, we feel it would be useful to present them in a form that is amenable to discussions later in this paper. In section 4, we present our results for LO and NLO cross sections, both for the differential distributions $d\sigma/d\log x$ and $d\sigma/d\log Q^2$, as well as the total cross section. This has been done for neutral as well as charged current cross sections. Section 5 has a short discussion on saturation and the final section makes a few concluding remarks.

2. Parton distributions

As already mentioned briefly in the introduction, deep inelastic scattering of UHE neutrinos is unique in the sense that it explores extreme regions of the (Q^2, x) phase space where no data from terrestrial accelerators exist to help with the nature of the distributions. We are therefore forced into making some assumptions regarding the nature of these distributions, particularly in the region of ultra low x and low Q^2 (the so-called saturation region), as well in the region of ultra low x and very high Q^2, for which too, no data exist. In what follows we shall expand a bit on this theme.

In the region between, say $50\,\mathrm{GeV}^2 < Q^2 < 10^5\,\mathrm{GeV}^2$, standard parametrisations are expected to work reasonably well. All parametrisations in these regions use parton densities of the form $Ax^\alpha(1-x)^\beta f(\sqrt{x})$ where the last function is some polynomial in $\sqrt{x}$. We have checked explicitly that all three of CTEQ5 [23], MRS99 [24] and GRV98 [25] parametrisations give very similar results within this region. However, the explicit parametrisation for either of CTEQ5 and MRS99 distributions do not work below $x < 10^{-5}$ whereas GRV98 allows x values up to 10^{-9}. For our numerical results, we therefore work with GRV98, except in the saturation region and the very large-Q^2 and small x region.

The region above $Q^2 = 10^6\,\mathrm{GeV}^2$ and low x ($x < 10^{-5}$) is beyond the region of validity of the *explicit parametrisations* of GRV98 (which is valid only up to $Q^2 = 10^6\,\mathrm{GeV}^2$). One option here is to use the starting distributions for GRV98 and evolve them (to LO or NLO order) into the above region. However, in this region, one also has the option of using an analytical form for the distribution function — the so-called double leading log (DLL) or Double Asymptotic Scaling (DAS) forms. In this approach, the DGLAP equations can be solved analytically, assuming that the evolution is driven by the splitting function P_{gg}. This was first shown in [26] and later developed for ultra-high energy neutrinos in [27]. A general review with calculational details may be found in [28]. This region is then matched appropriately at the boundary with GRV98. One could also use, other than variations of the DGLAP approach, the $\ln(1/x)$ resummation programme of BFKL or the unified DGLAP-BFKL treatment of [37]. The numerical changes are insignificant.

For the other region where the explicit GRV98 parametrisation is not valid, namely large Q^2 ($> 10^6\,\mathrm{GeV}^2$) and moderate x ($x > 10^{-5}$), one may again evolve the parton densities appropriately and then use them. However, numerically, it is simpler to just use GRV98 with a fixed value of $Q^2 = 10^6\,\mathrm{GeV}^2$, and, within this region, the error due to such an approach is negligible. It might seem counterintuitive that the final result depends negligibly on which resummation scheme is used in the ultra-low x and/or very high Q^2 scheme. However, as we show later in this paper, this simply follows from the fact that at these extreme (x, Q^2) values, the relative contribution in the integral (over x and Q^2) to the total cross section is already very small.

The summary of the various evolution equations and their applicable regions are shown in figure 1. We have used the leading log expressions for DAS; this is appropriate for matching with NLO GRV98.

Some comments regarding the saturation region are in order. In DIS at very low x and low Q^2, we find a high density of partons which is a non-perturbative system even though α_{s} may be small. There are essentially two approaches to high density QCD — the GLR [29] and Mueller, Qiu [30] aproach and the effective lagrangian method of McLerran and Venugopalan [31]. Using these two approaches a non-linear evolution equation has been developed by the Tel-Aviv group and a review may be found in their paper [32]. We have used saturated densities in the low x and low Q^2 region using this approach [33]. Some comments on the saturation region can be found later, in section 5.

3. NLO expressions for $\nu - N$ scattering

In this section we briefly review the $O(\alpha_{\mathrm{s}})$ (NLO) expressions for neutrino nucleon scattering. Many of these details may be found scattered in the literature — for example, see [39] — however it is convenient to write them down here in some detail, clearly demarcating the LO and NLO pieces. We will assume an isoscalar target N [$\equiv (p+n)/2$] as this is an excellent approximation to the typical neutrino detector material.

JHEP10(2002)012

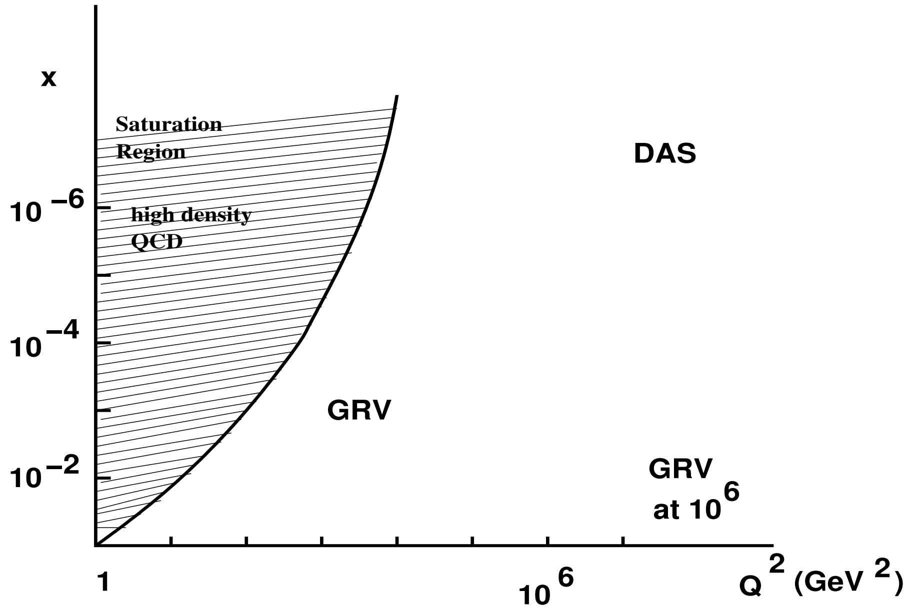

Figure 1: Summary of the parton distributions used in various regions DAS stands for double asymptotic scaling (or equivalently DLL or double leading log).

The general expression for the neutral current (NC) reaction

$$\overset{(-)}{\nu}_\mu N \longrightarrow \overset{(-)}{\nu}_\mu + \text{anything}$$

is given by

$$\frac{d^2\sigma^{(\nu,\bar{\nu})N}}{dxdy} = \frac{G_F^2}{2\pi}\left(\frac{M_Z^2}{Q^2+M_Z^2}\right)^2 s\left[\mathrm{F}_2(1-y) + \mathrm{F}_1 xy^2 \pm \mathrm{F}_3 xy\left(1-\frac{1}{2}y\right)\right], \tag{3.1}$$

where G_F is the Fermi coupling, M_Z the Z-boson mass and s the total centre-of-mass energy squared. The quantity Q^2 ($\equiv -q^2$) is the momentum transfer, the Bjorken variable $x = Q^2/(2p\cdot q)$ with p ($p^2 = M_p^2$) being the four momentum of the proton (or the isoscalar target) and $y \equiv Q^2/(xs)$.

The structure functions $\mathrm{F}_i \equiv \mathrm{F}_i(x, Q^2)(i = 1, 2, 3)$ are given by the convolution of bare parton distributions $q_i^{(0)}(y_p)$ and the partonic structure function $\hat{F}_i$. In other words,

$$\mathrm{F_i}(x, Q^2) = {q_j}^{(0)} \otimes \hat{F}_i^{q_j} + \bar{q}_j^{(0)} \otimes \hat{F}_i^{\bar{q}_j} + g^{(0)} \otimes \hat{F}_i^{g}\,, \tag{3.2}$$

where $\otimes$ denotes the convolution defined as

$${q_j}^{(0)} \otimes \hat{F}_i^{q_j} = \int_x^1 \frac{dy_p}{y_p} {q_j}^{(0)}(y_p)\hat{F}_i^{q_j}\left(\frac{x}{y_p}\right). \tag{3.3}$$

Denoting the generic weak interaction vertex involving a quark f by $\gamma^\mu(c_V^f \pm c_A^f\gamma_5)$, the leading order (LO) partonic structure functions are given by

$$\hat{F}_i^0(z) = K_i\delta(1-z)\,, \tag{3.4}$$

where $2K_1 = K_2 = ((c_V^f)^2 + (c_A^f)^2)$ and $K_3 = 2c_V^f c_A^f$. Clearly, $K_{1,2}$ correspond to parity conserving interactions whereas K_3 is a measure of parity violation. In the case of DIS, NLO corrections implies corrections to the parton structure functions coming from $\mathcal{O}(\alpha_s)$ corrections to the partonic cross sections.

For the quark initiated process, to order α_s, the partonic structure functions are given by

$$\hat{F}_i^q\left(z, Q^2\right) = K_i \left\{\delta(1-z) + \frac{2\alpha_s}{3\pi}\left[\zeta\; P_{qq}(z) + P_{qq}(z)\ln\left(\frac{Q^2}{\mu^2}\right) + C_i^q(z)\right]\right\}, \tag{3.5}$$

where the first term is the zeroth-order piece and the rest comprise the next-to-leading order corrections. The splitting function P_{qq} is defined through

$$P_{qq}(z) = \frac{(1+z^2)}{(1-z)_+} + \frac{3}{2}\delta(1-z)\,, \tag{3.6}$$

where the "plus prescription" is defined as usual. The renormalisation scale μ is introduced to make the coupling dimensionless in $n(=4+\epsilon)$ dimensions and

$$\zeta = \left[\frac{2}{n-4} + \gamma - \ln(4\pi)\right]. \tag{3.7}$$

Clearly, the collinear singularity manifests itself in the ζ dependent term in eq. (3.5) in the limit $\epsilon \to 0$. And, finally, the *coefficient functions* $C_i^q(z)$ are given by

$$\begin{aligned} C_i^q(z) =\; & (1+z^2)\left(\frac{\ln(1-z)}{(1-z)}\right)_+ - \frac{(1+z^2)}{(1-z)}\ln(z) - \\ & -\frac{3}{2}\frac{1}{(1-z)_+} + 3 + 2z - \delta(1-z)\left(\frac{9}{2} + \frac{\pi^2}{3}\right) + \Delta_i^q\,, \end{aligned} \tag{3.8}$$

with

$$\Delta_1^q = -2z\,, \qquad \Delta_2^q = 0\,, \qquad \Delta_3^q = -(1+z)\,. \tag{3.9}$$

For the gluon initiated process, on the other hand, the parton structure functions are given by

$$\hat{F}_i^g(z, Q^2) = K_i\frac{\alpha_s}{4\pi}\left[\zeta P_{gq}(z) + P_{gq}(z)\ln\left(\frac{Q^2}{\mu^2}\right) + C_i^g(z)\right], \tag{3.10}$$

where

$$P_{gq}(z) = (1-z)^2 + z^2\,; \tag{3.11}$$

and

$$C_i^g(z) = \{(1-z)^2 + z^2\}\ln\left(\frac{1-z}{z}\right) + 6z(1-z) + \Delta_i^g\,; \tag{3.12}$$

with

$$\Delta_1^g = 4z(1-z)\,, \qquad \Delta_2^g = \Delta_3^g = 0\,. \tag{3.13}$$

JHEP10(2002)012

Note that the gluonic contribution to F_3 vanishes identically. This feature follows from the $V - A$ structure of the weak interaction whereby the quark contribution is exactly opposite to the anti-quark contribution. For the anti-quark initiated processes all the structure functions are the same except for $\hat{F}_3^q(z, Q^2)$ which appears with the opposite sign in eq. (3.1). Absorbing the mass singularity into the bare parton distributions in the $\overline{MS}$ scheme, the Q^2 dependent structure functions can be expressed in terms of the renormalised parton distributions through

$$\begin{aligned} \mathrm{F}_1(x, Q^2) &= \sum_{j=1}^{n_f} K_{q_j}^{(pc)} \Big\{ \left(q_j\left(x, Q^2\right) + \bar{q}_j\left(x, Q^2\right)\right) + \\ &\qquad + \alpha_s(Q^2)\left[C_1^q(z) \otimes (q_j + \bar{q}_j) + 2C_1^g \otimes g\right] \Big\}, \end{aligned} \tag{3.14}$$

$$\begin{aligned} \mathrm{F}_2(x, Q^2) &= \sum_{j=1}^{n_f} K_{q_j}^{(pc)} x \Big\{ \left(q_j\left(x, Q^2\right) + \bar{q}_j\left(x, Q^2\right)\right) + \\ &\qquad + \alpha_s(Q^2)\left[C_2^q(z) \otimes (q_j + \bar{q}_j) + 2C_2^g \otimes g\right] \Big\}, \end{aligned} \tag{3.15}$$

$$\begin{aligned} \mathrm{F}_3(x, Q^2) &= \sum_{j=1}^{n_f} K_{q_j}^{(pv)} \Big\{ \left(q_j\left(x, Q^2\right) - \bar{q}_j\left(x, Q^2\right)\right) + \\ &\qquad + \alpha_s(Q^2)\left[C_3^q(z) \otimes (q_j - \bar{q}_j)\right] \Big\}. \end{aligned} \tag{3.16}$$

In eqs. (3.14), (3.15) and (3.16), the first term refers to the LO contribution to $\mathrm{F_i}(x, Q^2)$ whereas the second term is the pure NLO contribution. The superscripts *pc* and *pv* stand for "parity conserving" and "parity violating", respectively. The fact that the tree-level relation $F_2 = 2xF_1$ is no longer valid will play a key role in understanding some of the results detailed in the next section.

It is useful, at this stage, to note that for an isoscalar target we have

$$\begin{aligned} \sum_j^{n_f} K_{q_j}^{(pc)}\ (\mathrm{q}_j + \bar{\mathrm{q}}_j) &= \frac{1}{2}\left(K_u^{(pc)} + K_d^{(pc)}\right)\left(u + d + \bar{u} + \bar{d}\right) + \\ &\quad + K_d^{(pc)}\left(s + \bar{s} + b + \bar{b}\right) + K_u^{(pc)}\left(c + \bar{c} + t + \bar{t}\right), \\ \sum_j^{n_f} K_{q_j}^{(pv)}\ (\mathrm{q}_j - \bar{\mathrm{q}}_j) &= \frac{1}{2}\left(K_u^{(pv)} + K_d^{(pv)}\right)\ \left(u + d - \bar{u} - \bar{d}\right), \end{aligned} \tag{3.17}$$

where K_u and K_d are the couplings of the *up* and *down* type quark, respectively. All parton distributions are the "renormalised" parton distributions (i.e. $\mathrm{q}_j \equiv \mathrm{q}_j(x, Q^2)$).

The general expression for the charged current (CC) reaction

$$\overset{(-)}{\nu}_\mu N \longrightarrow \mu^\pm + \text{anything},$$

is given by

$$\frac{d^2\sigma^{(\nu,\bar{\nu})N}}{dxdy} = \frac{2G_F^2}{\pi}\left(\frac{M_W^2}{Q^2 + M_W^2}\right)^2 s\left[\mathrm{F}_2(1-y) + \mathrm{F}_1 xy^2 \pm \mathrm{F}_3 xy\left(1 - \frac{1}{2}y\right)\right], \tag{3.18}$$

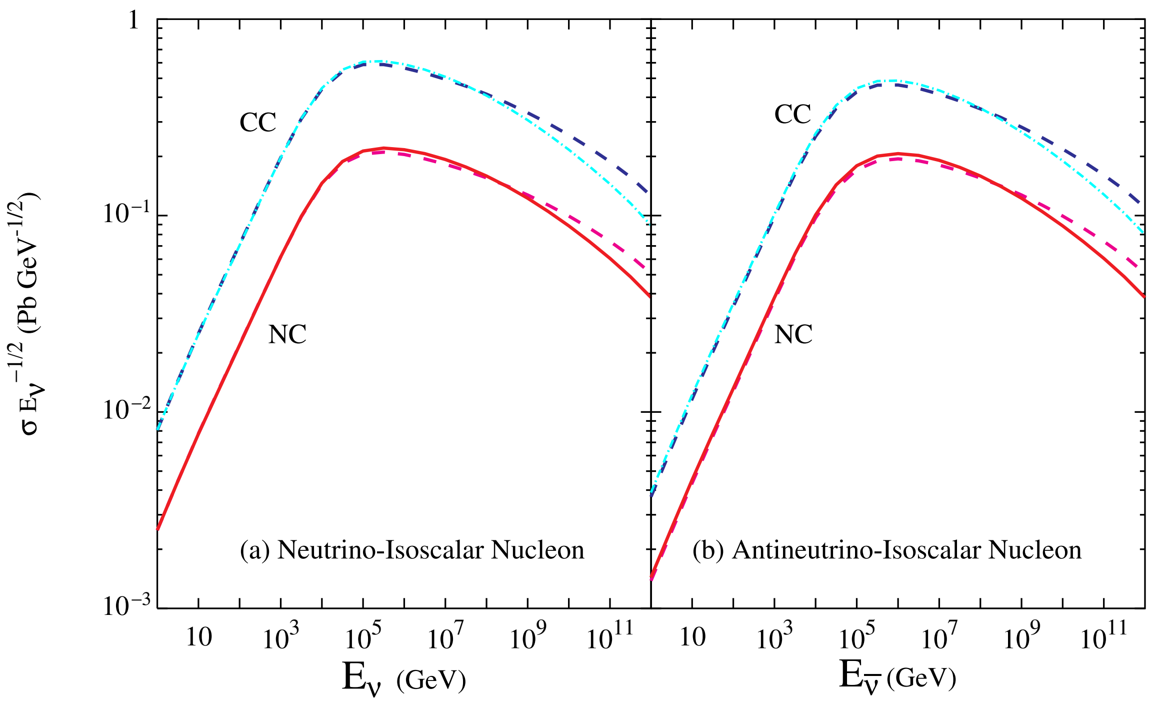

Figure 2: The total NC and CC cross sections as a function of the (anti-)neutrino energy.The left and right panels correspond to neutrino and antineutrino scattering, respectively.The solid (dashed) line represents the NLO (LO) cross sections.

all the notation being the same as NC. As the couplings K_i are now flavour independent ($2K_1 = K_2 = K_3 = 1/2$), they have been absorbed. For the isoscalar target, the quark distributions have the form

$$\sum_j^{n_f} (\mathrm{q}_j + \bar{\mathrm{q}}_j) = \frac{1}{2}\left(u + d + \bar{u} + \bar{d}\right) + (s + b + c + t)\,,$$
$$\sum_j^{n_f} (\mathrm{q}_j - \bar{q}_j) = \frac{1}{2}\left(u + d - \bar{u} - \bar{d}\right) + (s + b - c - t)\,. \qquad (3.19)$$

4. Results and discussion

Having set up the formalism, we now turn to an estimate of the numerical size of the NLO corrections. While the exact values of the cross sections for neutrino and antineutrino induced processes differ, (as also for charged-current and neutral-current interactions), one expects some similarities in the relative size of the corrections.

The total ν and $\bar{\nu}$ cross sections are displayed in figure 2. The rationale for choosing the particular scaling will become apparent as we progress. While the behaviour is essentially the same as that obtained by previous authors, the exact numbers (for the LO) differ marginally. The change is the result of our using a different set of parton distributions as compared to, say, ref. [16]. Moreover, we have taken care to use

Process	Order	$1\,\text{GeV} < E_\nu < 10^4\,\text{GeV}$		$10^7\,\text{GeV} < E_\nu < 10^{11}\,\text{GeV}$	
		$\mathcal{A}$	γ	$\mathcal{A}$	γ
ν-NC	LO	2.72×10^{-3}	0.945	1.17	0.390
	NLO	2.71×10^{-3}	0.945	2.06	0.360
$\bar{\nu}$-NC	LO	1.44×10^{-3}	0.964	1.16	0.391
	NLO	1.52×10^{-3}	0.963	2.06	0.360
ν-CC	LO	8.89×10^{-3}	0.940	3.57	0.383
	NLO	8.82×10^{-3}	0.941	6.50	0.349
$\bar{\nu}$-CC	LO	3.95×10^{-3}	0.961	2.85	0.386
	NLO	4.15×10^{-3}	0.960	5.18	0.353

Table 1: Parameters for the piecewise single power fit (see eq. (4.1)) for the cross sections in terms of the (anti-)neutrino energy.

the parton distributions appropriate for the order to which the partonic subprocesses are being calculated in each instance. To obtain a quantitative estimate of the differences in the total cross sections, it is useful to express them as a function of the neutrino energy. While a polynomial fit for $\log\sigma$ in terms of $\log E$ is straightforward, it is, unfortunately, not very illuminating. We attempt, instead, a piecewise fitting of the form

$$\sigma(\text{pb}) \approx \mathcal{A}\left(\frac{E_\nu}{1\,\text{GeV}}\right)^\gamma, \tag{4.1}$$

with the parameters $\mathcal{A}$ and γ as given in table 1. Thus, while σ grows almost linearly with E_ν for relatively small neutrino energies, the growth is tempered to $\sim E_\nu^{0.4}$ for larger E_ν. The particular scaling in figure 2, thus, serves to highlight the deviations at high energies from the exact scaling relation of eq. (4.1). Such a behaviour for the total cross section was found earlier, in [34], and as demonstrated there, it is the result of the fact that when the differential cross section is integrated over x and Q^2, the Q^2 integration is effectively cut-off at $Q^2 \simeq M_{Z,W}^2$ coupled with the fact that the number of valence quarks is finite. One might wonder at this stage at the apparent lack of unitarity reflected by the value of the exponent γ at high energies. In particular, in view of the rapidly rising parton distribution functions at low x predicted by all evolution equations, the question of the total cross section saturating the unitarity bound already at around $E_\nu \simeq 10^8\,\text{GeV}$ is a serious one that is addressed, for example, in refs. [15, 17].

While both figure 2 and table 1 seemingly demonstrate that, for small neutrino energies, the difference between the LO and the NLO cross sections is miniscule, the same certainly cannot be said of the results at large values of E_ν, This difference can be quantified in terms of the K-factor:

$$K = \frac{\sigma_{\text{NLO}}}{\sigma_{\text{LO}}}, \tag{4.2}$$

which we plot in figure 3.

JHEP10(2002)012

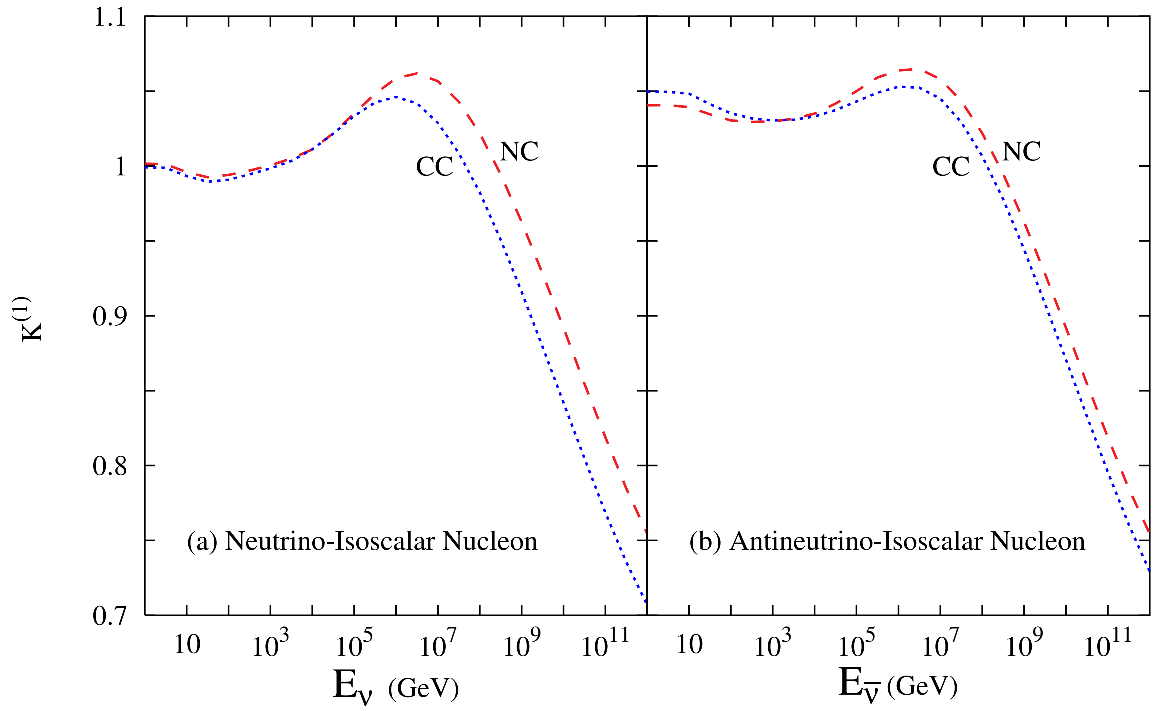

Figure 3: The ratio of the NLO to LO total NC and CC cross section as a function of (anti-)neutrino energy.

Various points are worthy of note here. As already anticipated, for small neutrino energies, the K-factor is remarkably close to one and confirms the usual belief that QCD corrections are unimportant. At larger energies ($E_\nu > 10^4$ GeV), the NLO contributions start to become important and the K-factor slowly grows to its maximum (~ 1.08) at about $E_\nu \sim 2 \times 10^6$ GeV. Thereafter, the $\sigma_{\rm NLO}$ grows slower with energy than does $\sigma_{\rm LO}$ (see table 1), resulting in a rather strong reduction of the K-factor by the time one reaches $E_\nu \simeq 10^{10}$ GeV.

4.1 ν-NC scattering

The reasons for the afore-mentioned behaviour of the K-factor are manifold and intertwined. Hence, before we attempt an understanding of this, it is perhaps more useful to look at the differential distributions. We begin by concentrating on the neutral current scattering process of neutrinos off isoscalar targets. In figure 4, we show the variation with Q^2 for three representative neutrino energies. The shape of the distributions are governed by both the dynamics as well as the parton densities. For low neutrino energies, the maximal energy transfer falls well short of M_Z and thus the neutrino-parton interaction is well described in terms of a 4-fermi interaction. As is well known, the cross section due to such an interaction lagrangian grows with the available center of mass energy.

On the other hand, the parton densities fall very sharply as the fraction of the proton energy they carry approaches unity. The interplay of these two effects leads to the skewed bell-like shape of the distribution. As the neutrino energy increases, so does the typical

JHEP10(2002)012

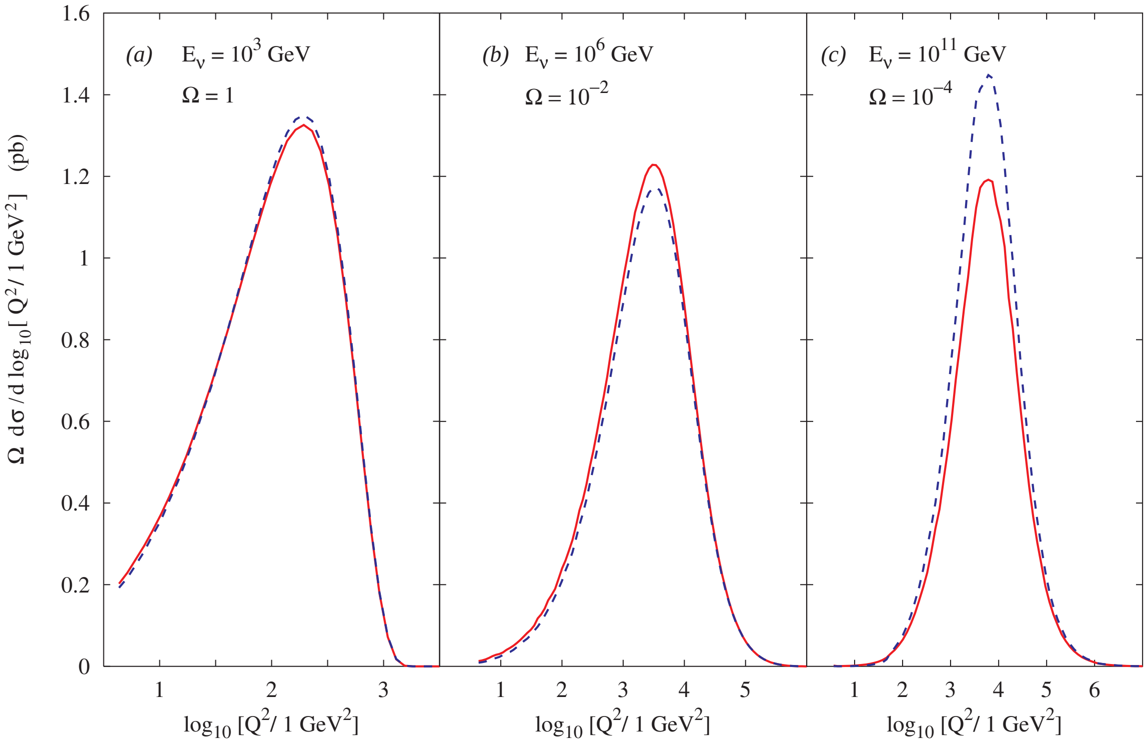

Figure 4: The differential NC cross section wrt $\log(Q^2)$ for three different neutrino energies. In each case, the solid (dashed) line give the NLO(LO) cross sections. The quantity Ω gives the factor by which the graphs have been scaled.

value of the neutrino-parton center of mass energy. Once this crosses $s \sim (100\,\mathrm{GeV})^2$, the natural scale of the problem, the contribution to the cross section is naturally dominated by virtual exchanges with $Q^2 \sim M_Z^2$. The skewness of the distribution is therefore removed to a large extent (see the central panel of figure 4). At even larger energies, this tendency is only reinforced.

The issues discussed above can also be understood in terms of distributions in the Bjorken variable x (see figure 5). With the fast fall of the parton densities at large x, it is only natural that such regions of the phase space should contribute very little to the cross section. This, of course, is reflected in the first two panels of figure 5. However, for very large E_ν, the situation is changed somewhat. Dynamics dictates that the region $Q^2 \sim M_Z^2$ (and, hence, relatively small x) receives prominence in the integration. As the maximum in distribution is still far away from $x \lesssim 1$, the aforementioned damping does not come into play and the fall-off is much smoother.

With these features in mind, we now return to the issue of the K-factor. To start with, let us re-examine figure 4, more particularly the last two panels where the deviation is more pronounced. Even a casual glance (and this is indeed borne out by a quantitative test) shows that the ratio of the NLO and LO differential cross sections is roughly constant over the significant range of Q^2. The shift from unity is as large as 25% for extremely large E_ν. As for the x distribution, a similar effect is in operation for not too large neutrino energies ($E_\nu \lesssim 10^8\,\mathrm{GeV}$). For progressively larger E_ν's though, the effect is concentrated more

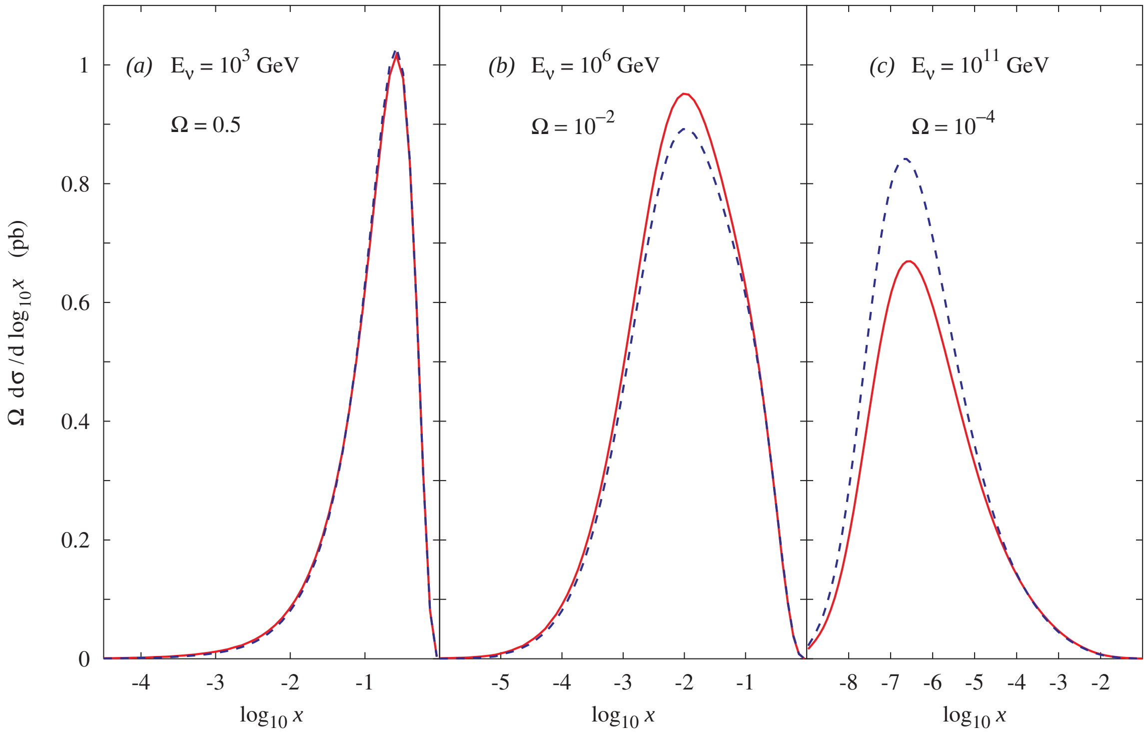

Figure 5: As in figure 4, but for variation in $\log(x)$ instead.

towards the peak in $\mathrm{d}\sigma/\mathrm{d}\log x$ (and may be as large as $\sim 30\%$). We may thus conclude that, while the NLO correction tends to be nearly independent of Q^2, it certainly does have a non-negligible variation in x, with the largest shifts occurring for $x \lesssim M_Z^2/(2M_p E_\nu)$. In other words, were we to consider the normalised differential distributions, the LO and NLO curves for $\mathrm{d}\sigma/\mathrm{d}\log Q^2$, for a given E_ν, would be virtually indistinguishable from each other, while those for $\mathrm{d}\sigma/\mathrm{d}\log x$ would seem laterally displaced, with the effect more pronounced for larger E_ν.

The various contributions to the K-factor are often separated (albeit not in a strictly gauge-invariant way) into two parts: those arising from the differences in the LO and the NLO parton distributions and those that are due to the changes in the partonic cross sections. In figure 6 we display the effects of such a division. This would also serve to facilitate a comparison of our results with those available in the literature. As is seen readily, ignoring the corrections to the lowest order partonic cross sections but using the NLO distributions would have led to a much steeper suppression for larger neutrino energies. The main reason for the fall is that while at large E_ν and hence large s, x is small and hence the partonic distributions are large, the rise of the distributions is *steeper* for LO than for NLO. (This is, of course, a well known fact and arises because, at NLO, the splitting function (say P_{qg}) has a $1/x$ singularity at $\mathcal{O}(\alpha_s)$ which needs to be stemmed by choosing flatter distributions at a given energy compared to the LO case. Put differently, a stable evolution of, say, F_2 requires that the NLO steepness of P_{qg} has to be compensated by a gluon density which is less steep at NLO than at LO. It is for this reason that the starting distributions for LO and NLO are always substantially different). In the literature

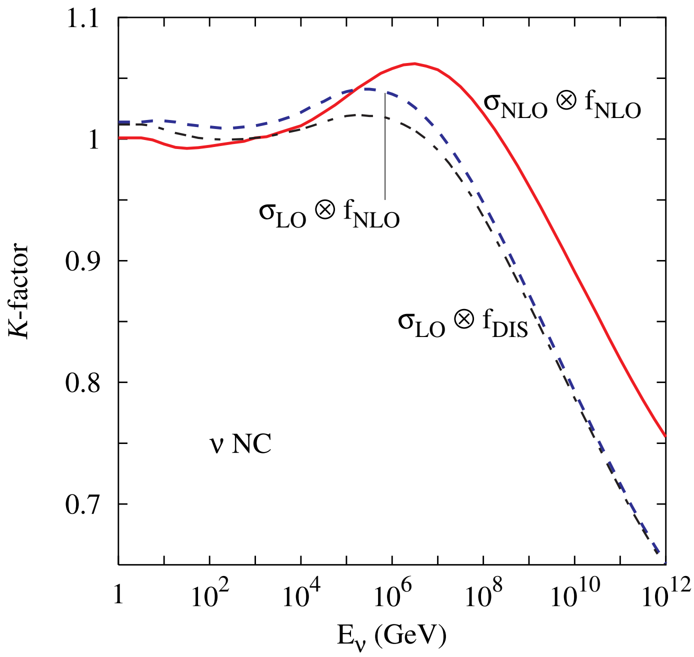

Figure 6: A comparison of the true K-factor (solid line) for the neutrino-nucleon neutral current process and that obtained if the leading order cross sections were convoluted with the NLO ($\overline{\mathrm{MS}}$) parton distributions (dashed line) or the DIS ones (dotted line).

(for example, ref. [16]), it has often been claimed that using the LO partonic cross section convoluted with the partonic distributions in the DIS scheme is an effective method for approximating the magnitude of the full NLO corrections. However, as figure 6 clearly shows this is not the case and the "true" NLO corrections (wherein the NLO partonic cross section is convoluted with the NLO distributions), gives a result very different from using just the LO partonic cross section convoluted with either the NLO $\overline{MS}$ distribution or the distributions in the DIS scheme.

Having understood a decreasing K-factor for high neutrino energies, we now turn to the presence of a maximum. For sufficiently small E_ν's, when x is not too small (see figure 5), the gluon, which is what may make the NLO large at small x, is still to kick in, and the LO and NLO curves for the total cross section start out virtually together. As we move to larger values of E_ν, and hence smaller x, the gluon density itself becomes larger. Consequently, $\sigma_{\rm NLO}$ increases faster than $\sigma_{\rm LO}$. For even higher E_ν's, the bulk of the contribution comes from progressively smaller x and the fact of the LO distributions being larger, at small x, than the NLO ones becomes the overriding factor; the rise in $\sigma_{\rm NLO}$ is suppressed.

Before concluding this section, we would like to recall that whereas the gluon is the main contributing factor in the NLO graphs, no gluon appears in the initial state in the LO case. However, even for the LO, the gluon manifests itself, indirectly, through large values of the sea quark distributions. The inclusion of the NLO contribution only serves to ameliorate this suppression. It is interesting to note that the "extra" piece may contribute as much as 10% to the cross section and is, by no means, negligible.

4.2 The $\bar{\nu}$-NC and the CC cross-sections

Having discussed the ν-NC interaction in detail, we now comment on the other interactions that we have briefly discussed above. As both figures 2 and 3 show, the main features are quite similar and it is the small differences that we concentrate on here. Starting with the $\bar{\nu}$-NC process, note that the K-factor at large energies is nearly the same as that for the corresponding ν-NC interaction. While the value at the peak ($E_{\bar{\nu}} \sim 10^6\,\mathrm{GeV}$) is also approximately the same, the dip at lower energies is far more gradual. Even more striking, at low energies $E_{\bar{\nu}} \lesssim 10\,\mathrm{GeV}$) is that the K-factor is discernibly different from unity. This difference is but an example of the afore-mentioned subtle interplay between the parton-level cross-sections and the parton densities. At the partonic level, the only difference between the ν-NC and the $\bar{\nu}$-NC cross sections lies in the reversal of the sign of the structure function F_3, which in turn, is controlled by the valence quarks. At small energies, most of the contribution to the total cross section comes from the valence quarks and hence this extra additive piece has a significant role to play (and, indeed, is responsible for the difference in ν-NC and $\bar{\nu}$-NC cross sections). This relative shift is less pronounced for the NLO, as the F_3 contribution is now smaller while the combined F_1 and F_2 contribution is marginally larger — again, a consequence of the interplay between the parton-level cross sections and the shape of the parton densities themselves. With the increase of the (anti-)neutrino energy the peak in $\mathrm{d}\sigma/\mathrm{d}\log x$ shifts to progressively smaller values of x (see figure 5), thereby rendering the F_3 contribution insignificant.

As for the charged current processes, it is easy to see that the NLO corrections are quite analogous to the cases already considered. Thus, notwithstanding the difference in the absolute value of the cross sections, the K-factor is expected to be similar, and this indeed is attested to by figure 3. There is a minor difference though. Unlike the case for the NC processes, at high energies, the K-factors for the neutrino- and antineutrino-induced CC processes are no longer the same. This has its origin in the expression for the F_3 term as applied to CC (see eq. (3.19)). At high energies (and, hence, low x), the F_3 contribution is now nearly proportional to the strange sea content in the nucleon. As the latter is, by no means, small at such low x values, the differences in the absolute values of the cross sections as well as in the K-factors are expected.

4.3 Observables "stable" under QCD corrections

We have seen that all the four relevant cross sections receive significant corrections at the NLO level. Moreover, the corrections are not easy to parametrise as a function of energy. Added to this are dependencies on the parton distributions used. It is therefore of interest to inquire if there exist observables that are relatively insensitive to such corrections, not the least for their usefulness in searches for new physics. One such observable is the ratio of σ_ν^{CC} and $\sigma_{\bar{\nu}}^{\mathrm{CC}}$ (the corresponding ratio for the NC cross sections is not a measurable for cosmic neutrinos). In figure 7a, we exhibit this ratio as a function of the (anti-)neutrino energy. Since the bulk of the NLO corrections are common to the two cross sections under discussion, the ratio, as expected, changes little when these corrections are included.

JHEP10(2002)012

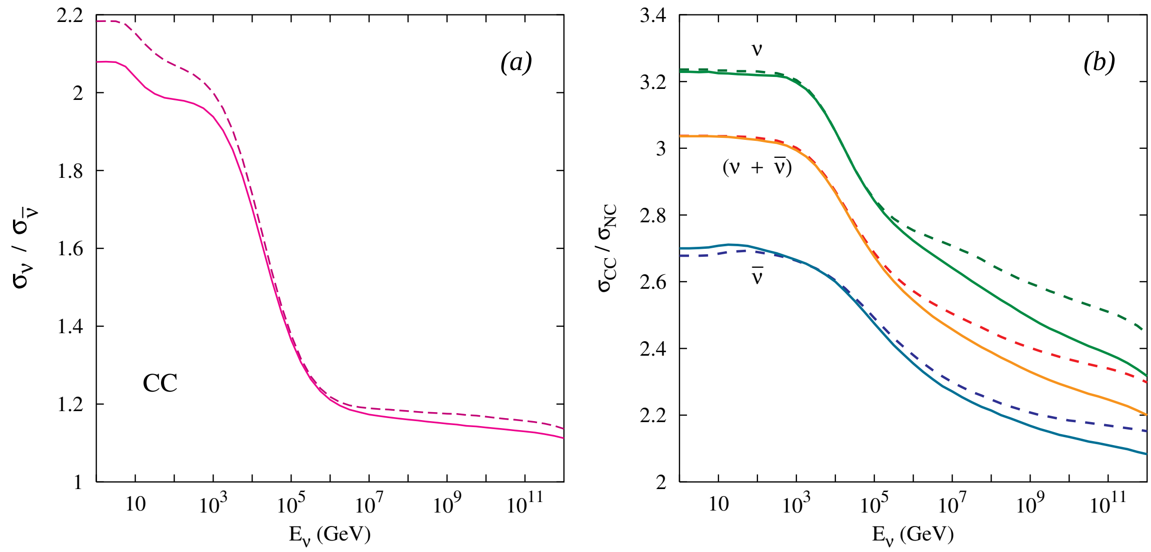

Figure 7: (a) The ratio of the charged-current cross sections for a neutrino and an antineutrino scattering off an isoscalar nucleon; (b) the ratio of charged-current and neutral current cross sections for a neutrino, an antineutrino and a beam composed of equal number of neutrinos and antineutrinos. In either case, the solid (dashed) lines correspond to the NLO (LO) cross sections.

Unfortunately, in the context of an actual experiment, the ratio above would be measurable only in the presence of a substantial magnetic field, and is hence of limited use as far as a neutrino telescope is concerned. However, the ratio of charged current and neutral current cross sections is measurable, and can indeed be a good discriminator in the search for new physics [18]. As figure 7b shows, this ratio, again, is far less sensitive to QCD corrections than are the individual cross sections.

5. Saturation effects

We have seen in the earlier section the complex interplay between partonic cross sections and the evolution of partonic densities at LO and NLO.

However, there is another issue which is of importance in this process. At the extremely low values of x that we are considering, the proton is a dense collection of partons and saturation effects are expected to come into play. Typically, this happens when recombination effects from $g\,g \to g$ start having a discernible effect. Such processes are expected to slow down the usual rise of the gluon distribution predicted by DGLAP evolution and is expected to take place around a scale

$$Q_s^2 = (1\,\mathrm{GeV})^2 \left(\frac{x_0}{x}\right)^\lambda . \tag{5.1}$$

The parameters λ and x_0 as fitted to HERA data are found to be $\lambda = 0.288$ and $x_0 = 3.04 \times 10^{-4}$ [17, 35]. Around $x \simeq 10^{-8}$ this works out to $Q_s^2 \simeq 20\,\mathrm{GeV}^2$. As is clear from the above, at larger values of x, saturation is expected to set in at even lower scales.

Keeping this in mind, we have smoothly interpolated, in the low Q^2 ($\lesssim 50\,\mathrm{GeV}^2$) and low x ($\lesssim 10^{-6}$) region, from GRV98 to the saturation model mentioned in the introduction [32]. All the graphs and the analyses discussed in this paper are based on interpolation of densities shown in figure 1.

While this is, of course, the consistent way of doing this, a useful exercise would be to estimate the effect of these saturation models on our results. To this end, we substituted the saturation model in the low x and Q^2 region by the standard GRV98 evolution and compared the results. We find that the effect of saturation, in the total cross section is negligible and, at its largest, is of the order of around 0.2%. The reason for this is not far to seek. In the large range of x and Q^2 values that we are spanning in our integrals, the saturation region accounts for an exceptionally tiny part of the phase space and consequently, has little effect on the final result. The physical requirement of saturation is however, an important one for many reasons, not least in stemming the rise of the distributions at ultra low x and thereby preventing the cross section from crossing the unitarity bound. As mentioned earlier, we will not discuss this aspect here, but refer the reader to refs. [15, 17].

6. Conclusions

In this paper, we have explicitly calculated the NLO (i.e. $\mathcal{O}(\alpha_\mathrm{s})$) corrections to ultra high energy neutrino-proton (or isoscalar nucleon) scattering. We have identified the various regions in the x-Q^2 space where different parametrisations of the quark and gluon densities are valid and discussed the contributions of each of these regions. In particular, we have carefully looked at the low Q^2 and ultra low x region and discussed the effect of saturation in this region and found it to have a very small effect on the overall NLO behaviour. We have also calculated the size of the NLO corrections compared with the LO (the K-factor) and tried to give a qualitative explanation for the results.

It is clear from our analysis that the higher order corrections are not small — in fact the NLO in a certain region substantially brings *down* the LO cross section and we have explained in the text why this happens. It is clear from our analysis that NLO calculations are necessary for UHE neutrino isoscalar scattering processes to get a complete picture, not least for isolating the QCD effects from those due to possible physics beyond the s tandard model.

We have also discussed briefly, observables that are insensitive to higher order corrections. Such observables, which are "stable" under QCD corrections would be useful discriminators in the search for new physics.

At this point, one should also perhaps consider how our results would change if one were to use other evolution equations like BFKL [36] or the unified BFKL-DGLAP equation of [37]. There have also been attempts to use the BFKL power law rise of the structure function and relate this power to the average inelasticity [38]. These approaches are relevant in the ultra low x regions that we are discussing. However, as has been shown in [34], resumming leading and non-leading $\ln(1/x)$ effects through the above equations gives neutrino cross sections which are compatible with those obtained from the NLO DGLAP

JHEP10(2002)012

framework, thereby reducing potential ambiguities in the extrapolation of the cross section from the (x, Q^2) domain of terrestrial accelerators (particularly HERA) to the ultra low x region that are explored by UHE neutrinos.

It is possible now to look at the next order in α_s (NNLO) to see what effect this has at least upto values of $x \simeq 10^{-4}$ [40]. This is the subject of a future study.

Acknowledgments

One of us (R.B.) would like to thank Uri Maor and Eran Naftali for useful discussions and providing us with the interpolation program for densities in the saturation region. We would also like to thank V. Ravindran for useful discussions. D.C. thanks the Dept. of Science and Technology, India for financial assistance under the Swarnajayanti Fellowship grant.

References

[1] P.W. Gorham, K.M. Liewer and C.J. Naudet, *Initial results from a search for lunar radio emission from interactions of* $\geq 10^{19}\,eV$ *neutrinos and cosmic rays*, in proceedings *26th Inter. Cosmic Ray Conf.*, Utah, 1999 [astro-ph/9906504];
P.W. Gorham, K.M. Liewer, C.J. Naudet, D.P. Saltzberg and D.R. Williams, *Radio limits on an isotropic flux of* $> 100\,eeV$ *cosmic neutrinos*, in proceedings *First Inter. Workshop on radio detection of high-energy particles*, Amer. Inst. of Phys., 2001 [astro-ph/0102435] and at http://www.physics.ucla.edu/~moonemp/radhep/workshop.html.

[2] R.J. Protheroe and P.A. Johnson, *Propagation of ultrahigh-energy protons over cosmological distances and implications for topological defect models*, *Astropart. Phys.* **4** (1996) 253 [astro-ph/9506119].

[3] P. Bhattacharjee and G. Sigl, *Origin and propagation of extremely high energy cosmic rays*, *Phys. Rept.* **327** (2000) 109 [astro-ph/9811011].

[4] Y. Totsuka, *Neutrino astronomy*, *Rep. Prog. Phys.* **55** (1992) 377;
T.K. Gaisser, F. Halzen and T. Stanev, *Particle astrophysics with high-energy neutrinos*, *Phys. Rept.* **258** (1995) 173 [hep-ph/9410384];
J.N. Bahcall et al., *Progress and prospects in neutrino astrophysics*, *Nature* **375** (1995) 29 [astro-ph/9503047];
S. Barwick, F. Halzen and P.B. Price, *The search for neutrino sources beyond the sun*, *Int. J. Mod. Phys.* **A 11** (1996) 3393 [astro-ph/9512079].

[5] THE AMANDA collaboration, G.C. Hill, *Results from Amanda*, astro-ph/0106064 http://amanda.berkeley.edu/;
A similar, though now defunct effort is the Deep Undersea Muon and Neutrino Detection (DUMAND) experiment http://dumand.phys.washington.edu/~dumand/.

[6] BAIKAL collaboration, V.A. Balkanov et al., *The lake Baikal experiment: selected results*, astro-ph/9906255, for general information, see http://www.ifh.de/baikal/baikalhome.html.

[7] ANTARES collaboration, E. Aslanides et al., *A deep sea telescope for high energy neutrinos*, astro-ph/9907432, http://antares.in2p3.fr/antares/antares.html.

[8] http://www.roma1.infn.it/nestor/nestor.html.

[9] AMANDA collaboration, E. Andres et al., *Amanda: status, results and future*, astro-ph/9906205, http://www.ps.uci.edu/~icecube/workshop.html.

[10] http://kuhep4.phsx.ukans.edu/~iceman/index.html.

[11] J.J. Blanco-Pillado, R.A. Vázquez and E. Zas, *Limits on topological defect neutrino fluxes from horizontal air shower measurements*, *Phys. Rev. Lett.* **78** (1997) 3614 [astro-ph/9612010];
K.S. Capelle, J.W. Cronin, G. Parente and E. Zas, *On the detection of ultra high energy neutrinos with the Auger observatory*, *Astropart. Phys.* **8** (1998) 321 [astro-ph/9801313];
A. Letessier-Selvon, *Establishing the GZK cutoff with ultra high energy tau neutrinos*, *AIP Conf. Proc.* **566** (2000) 157 [astro-ph/0009444];
D. Fargion, *Discovering ultra high energy neutrinos by horizontal and upward tau air-showers: first evidences in terrestrial gamma flashes*, *Astrophys. J.* **570** (2002) 909 [astro-ph/0002453];
X. Bertou, P. Billoir, O. Deligny, C. Lachaud and A. Letessier-Selvon, *Tau neutrinos in the auger observatory: a new window to UHECR sources*, *Astropart. Phys.* **17** (2002) 183 [astro-ph/0104452];
J.L. Feng, P. Fisher, F. Wilczek and T.M. Yu, *Observability of earth-skimming ultra-high energy neutrinos*, *Phys. Rev. Lett.* **88** (2002) 161102 [hep-ph/0105067];
A. Kusenko and T.J. Weiler, *Neutrino cross sections at high energies and the future observations of ultrahigh-energy cosmic rays*, *Phys. Rev. Lett.* **88** (2002) 161101 [hep-ph/0106071].

[12] J.F. Ormes et al., in proceedings *25th international cosmic ray conference*, M.S. Potgieter et al. eds., Durban, 1997, vol. 5, p. 273;
Y. Takahashi et al., in proceedings of *International symposium on extremely high energy cosmic rays: astrophysics and future observatories*, M. Nagano ed., Institute for Cosmic Ray Research, Tokyo, 1996, p. 310;
D.B. Cline and F.W. Stecker, *Exploring the ultrahigh energy neutrino universe*, astro-ph/0003459;
see also http://lheawww.gsfc.nasa.gov/docs/gamcosray/hecr/OWL/.

[13] See http://www.ifcai.pa.cnr.it/Ifcai/euso.html.

[14] See http://www.phys.hawaii.edu/~gorham.

[15] D.A. Dicus, S. Kretzer, W.W. Repko and C. Schmidt, *Ultrahigh-energy neutrino nucleon cross-sections and perturbative unitarity*, *Phys. Lett.* **B 514** (2001) 103 [hep-ph/0103207].

[16] R. Gandhi, C. Quigg, M.H. Reno and I. Sarcevic, *Neutrino interactions at ultrahigh energies*, *Phys. Rev.* **D 58** (1998) 093009 [hep-ph/9807264].

[17] M.H. Reno, I. Sarcevic, G. Sterman, M. Stratmann and W. Vogelsang, *Ultrahigh energy neutrinos, small x and unitarity*, hep-ph/0110235.

[18] M. Carena, D. Choudhury, S. Lola and C. Quigg, *Manifestations of R-parity violation in ultrahigh-energy neutrino interactions*, *Phys. Rev.* **D 58** (1998) 095003 [hep-ph/9804380].

[19] G. Sigl, S. Lee, D.N. Schramm and P. Coppi, *Cosmological neutrino signatures for grand unification scale physics*, *Phys. Lett.* **B 392** (1997) 129 [astro-ph/9610221];
M.A. Doncheski and R.W. Robinett, *Leptoquark production in ultrahigh-energy neutrino interactions revisited*, *Phys. Rev.* **D 56** (1997) 7412 [hep-ph/9707328];
L. Brucher, P. Keranen and J. Maalampi, *Searching scalar resonances with ultra-high energy neutrinos*, *J. High Energy Phys.* **05** (2001) 060 [hep-ph/0011138].

[20] S. Nussinov and R. Shrock, *Some remarks on theories with large compact dimensions and TeV-scale quantum gravity*, *Phys. Rev.* **D 59** (1999) 105002 [hep-ph/9811323]; *On high-energy behavior of cross sections in theories with large extra dimensions*, *Phys. Rev.* **D 64** (2001) 047702 [hep-ph/0103043];
R.V. Konoplich and S.G. Rubin, *Possible signature of low scale gravity in ultra high energy cosmic rays*, *Sov. Phys. JETP Lett.* **72** (2000) 97 [astro-ph/0005225];
P. Jain, D.W. McKay, S. Panda and J.P. Ralston, *Extra dimensions and strong neutrino nucleon interactions above $10^19\,eV$: breaking the GZK barrier*, *Phys. Lett.* **B 484** (2000) 267 [hep-ph/0001031];
F. Cornet, J.I. Illana and M. Masip, *TeV strings and the neutrino nucleon cross section at ultra-high energies*, *Phys. Rev. Lett.* **86** (2001) 4235 [hep-ph/0102065];
A. Goyal, A. Gupta and N. Mahajan, *Neutrinos as source of ultra high energy cosmic rays in extra dimensions*, *Phys. Rev.* **D 63** (2001) 043003 [hep-ph/0005030];
S.I. Dutta, M.H. Reno and I. Sarcevic, *On black hole detection with the owl/airwatch telescope*, *Phys. Rev.* **D 66** (2002) 033002 [hep-ph/0204218];
A. Jain, P. Jain, D.W. McKay and J.P. Ralston, *Graviton enhanced UHE neutrino cross-sections and giant air showers*, *Int. J. Mod. Phys.* **A 17** (2002) 533;
A. Ringwald and H. Tu, *Collider versus cosmic ray sensitivity to black hole production*, *Phys. Lett.* **B 525** (2002) 135 [hep-ph/0111042];
R. Emparan, M. Masip and R. Rattazzi, *Cosmic rays as probes of large extra dimensions and TeV gravity*, *Phys. Rev.* **D 65** (2002) 064023 [hep-ph/0109287];
L. Anchordoqui and H. Goldberg, *Experimental signature for black hole production in neutrino air showers*, *Phys. Rev.* **D 65** (2002) 047502 [hep-ph/0109242];
J. Alvarez-Muniz, F. Halzen, T. Han and D. Hooper, *Phenomenology of high energy neutrinos in low-scale quantum gravity models*, *Phys. Rev. Lett.* **88** (2002) 021301 [hep-ph/0107057];
M. Kowalski, A. Ringwald and H. Tu, *Black holes at neutrino telescopes*, *Phys. Lett.* **B 529** (2002) 1 [hep-ph/0201139].

[21] J. Alvarez-Muniz, F. Halzen and D.W. Hooper, *High energy neutrinos from gamma ray bursts: event rates in neutrino telescopes*, *Phys. Rev.* **D 62** (2000) 093015 [astro-ph/0006027];
S.I. Dutta, M.H. Reno and I. Sarcevic, *Tau-neutrinos underground: signals of $\nu_\mu \to \nu_\tau$ oscillations with extragalactic neutrinos*, *Phys. Rev.* **D 62** (2000) 123001 [hep-ph/0005310]; *High energy neutrino signals of four neutrino mixing*, *Phys. Rev.* **D 64** (2001) 113015 [hep-ph/0104275];
I.F.M. Albuquerque and G.F. Smoot, *Measuring atmospheric neutrino oscillations with neutrino telescopes*, *Phys. Rev.* **D 64** (2001) 053008 [hep-ph/0102078];
S. Bottai and S. Giurgola, *Uhe and ehe neutrino induced taus inside the earth*, astro-ph/0205325;
J.F. Beacom, P. Crotty and E.W. Kolb, *Enhanced signal of astrophysical tau neutrinos propagating through earth*, *Phys. Rev.* **D 66** (2002) 021302 [astro-ph/0111482].

[22] P. Jain, J.P. Ralston and G.M. Frichter, *Neutrino absorption tomography of the earth's interior using isotropic ultra-high energy flux*, *Astropart. Phys.* **12** (1999) 193 [hep-ph/9902206];
M. Lindner, T. Ohlsson, R. Tomas and W. Winter, *Tomography of the earth's core using supernova neutrinos*, hep-ph/0207238.

[23] CTEQ collaboration, H.L. Lai et al., *Global QCD analysis of parton structure of the nucleon: CTEQ5 parton distributions*, *Eur. Phys. J.* **C 12** (2000) 375 [hep-ph/9903282].

[24] A.D. Martin, R.G. Roberts, W.J. Stirling and R.S. Thorne, *Parton distributions and the LHC: W and Z production*, *Eur. Phys. J.* **C 14** (2000) 133 [hep-ph/9907231].

[25] M. Glück, E. Reya and A. Vogt, *Dynamical parton distributions revisited*, *Eur. Phys. J.* **C 5** (1998) 461 [hep-ph/9806404].

[26] A. De Rujula, S.L. Glashow, H. David Politzer, S.B. Treiman, Frank Wilczek, and A. Zee, *Possible nonregge behavior of electroproduction structure functions*, *Phys. Rev.* **D 10** (1974) 1649.

[27] D.W. McKay and J.P. Ralston, *Small-x QCD and the ultrahigh-energy neutrino n total cross-section*, *Phys. Lett.* **B 167** (1986) 103;
G.M. Frichter, D.W. McKay and J.P. Ralston, *Prediction on the ultrahigh energy neutrino nucleon cross section from new structure function data at small x*, *Phys. Rev. Lett.* **74** (1995) 1508 [hep-ph/9409433], erratum *ibid.* **77** (1996) 4107.

[28] For a review, see, S. Forte and R.D. Ball, *Universality and scaling in perturbative QCD at small x*, *Acta Phys. Polon.* **B26** (1995) 2097 [hep-ph/9512208].

[29] L.V. Gribov, E.M. Levin and M.G. Ryskin, *Semihard processes in QCD*, *Phys. Rept.* **100** (1983) 1.

[30] A.H. Mueller and J.-w. Qiu, *Gluon recombination and shadowing at small values of x*, *Nucl. Phys.* **B 268** (1986) 427.

[31] L.D. McLerran and R. Venugopalan, *Computing quark and gluon distribution functions for very large nuclei*, *Phys. Rev.* **D 49** (1994) 2233 [hep-ph/9309289]; *Green's functions in the color field of a large nucleus*, *Phys. Rev.* **D 50** (1994) 2225 [hep-ph/9402335]; *Fock space distributions, structure functions, higher twists and small x*, *Phys. Rev.* **D 59** (1999) 094002 [hep-ph/9809427].

[32] E. Gotsman et al., *High density QCD at thera*, hep-ph/0101344.

[33] E. Naftali, private communication.

[34] J. Kwiecinski, A.D. Martin and A.M. Stasto, *Penetration of the earth by ultrahigh energy neutrinos predicted by low x QCD*, *Phys. Rev.* **D 59** (1999) 093002 [astro-ph/9812262].

[35] K. Golec-Biernat and M. Wusthoff, *Saturation effects in deep inelastic scattering at low Q^2 and its implications on diffraction*, *Phys. Rev.* **D 59** (1999) 014017 [hep-ph/9807513]; *Saturation in diffractive deep inelastic scattering*, *Phys. Rev.* **D 60** (1999) 114023 [hep-ph/9903358].

[36] E.A. Kuraev, L.N. Lipatov and V.S. Fadin, *The Pomeranchuk singularity in nonabelian gauge theories*, *Zh. Eksp. Teor. Fiz.* **72** (1977) 377;
Ya.Ya. Balitzkij and L.N. Lipatov, *The Pomeranchuk singularity in quantum chromodynamics*, *Yad. Fiz.* **28** (1978) 1597;
J.B. Bronzan and R.L. Sugar, *Regge behavior of spontaneously broken nonabelian gauge theory*, *Phys. Rev.* **D 17** (1978) 585;
T. Jaroszewicz, *Infrared divergences and Regge behavior in QCD*, *Acta Phys. Polon.* **B11** (1980) 965.

[37] J. Kwiecinski, A.D. Martin and A.M. Stasto, *A unified BFKL and glap description of F_2 data*, *Phys. Rev.* **D 56** (1997) 3991 [hep-ph/9703445]; *A unified BFKL and DGLAP evolution equation for quarks and gluons*, *Acta Phys. Polon.* **B28** (1997) 2577.

[38] J.A. Castro Pena, G. Parente and E. Zas, *Measuring the BFKL pomeron in neutrino telescopes*, *Phys. Lett.* **B 500** (2001) 125 [hep-ph/0011043].

[39] B. Humpert and W.L. van Neerven, *Nucl. Phys.* **B 184** (1981) 225.

[40] See, for example, W.L. van Neerven and A. Vogt, *Parton densities and structure functions at next-to-next-to-leading order and beyond*, *J. Phys.* **G 28** (2002) 727 [hep-ph/0107194].

JHEP10(2002)012